Stephan Heinitz*, Emilio A. Maugeri, Dorothea Schumann, Rugard Dressler, Niko Kivel, Carlos Guerrero, Ullrich Köster, Moshe Tessler, Michael Paul, Shlomi Halfon and the n_TOF Collaboration[a]

Production, separation and target preparation of ^{171}Tm and ^{147}Pm for neutron cross section measurements

DOI 10.1515/ract-2016-2728
Received November 8, 2016; accepted March 6, 2017; published online April 14, 2017

Abstract: The knowledge of the neutron capture cross sections of s-process branching point isotopes represents a basic requirement for the understanding of star evolution. Since such branching point isotopes are by definition radioactive, the measurement of their cross sections from thermal to stellar energies becomes a challenging task. Considerable amounts of material have to be produced, representing a significant radioactive hazard. We report here on the production and separation of 3.5 mg ^{171}Tm from 240 mg $^{170}Er_2O_3$ and 72 µg ^{147}Pm from 100 mg $^{146}Nd_2O_3$ irradiated at the ILL high flux reactor. Thin targets were prepared with high chemical and radioisotopic purity suitable for neutron capture measurements at n_TOF CERN and the SARAF-LiLiT facility.

Keywords: Lanthanide separation, ^{171}Tm, ^{147}Pm, radioactive target, neutron capture cross section.

1 Introduction

The origin of all elements heavier than Li relies on processes occurring during stellar evolution. Depending on the physical parameters describing a star, several processes of nuclear synthesis have been postulated to account for the abundance of elements in the Universe [1]. For massive stars in the asymptotic giant branch (AGB) stage, the main synthesis pathway is represented by the so-called s-process, where mainly elements heavier than Fe are produced by a series of neutron captures and subsequent β-decays close to the stability line. In order to understand the nature of this process, the knowledge of neutron cross sections at stellar energies for all involved isotopes is mandatory. This is especially important for those isotopes, where neutron capture and β-decay compete, since here a branching towards a higher or lower neutron number becomes possible. This circumstance is illustrated in Figure 1, where the production and destruction pathway for nuclides with mass number A = 147 and A = 171 is shown. The scientific community has issued a list of the 21 most important of such branching point isotopes, where a measurement of the neutron capture cross section is of great significance ([2] – see especially table 3).

Since all branching point isotopes are radioactive, their production, handling and measurement represent a challenging endeavor. Thus, only two of the above mentioned 21 radioactive nuclides have been successfully measured at neutron time-of-flight facilities so far – ^{151}Sm [3] and ^{63}Ni [4, 5]. The isotope ^{171}Tm had already been subjected to investigations at the LANSCE time-of-flight facility at Los Alamos, USA [6, 7]. However, the investigators reported difficulties of poor counting statistics and high background, which they attributed to an unexpectedly high content of stable ^{169}Tm in their final target. Their experimental activities on ^{171}Tm have been recently resumed [8, 9]. Nevertheless, no successful measurement of the cross section of ^{147}Pm or ^{171}Tm in the range from thermal to stellar neutron energies was reported until now. So far, experimental information for the (n, γ) cross sections of ^{147}Pm and ^{171}Tm was only obtained by neutron activation in a quasi-stellar spectrum at 25 keV [6, 10].

In this paper, we report on the separation of ^{171}Tm and ^{147}Pm and the target production containing these isotopes.

[a]www.cern.ch/ntof

***Corresponding author: Stephan Heinitz,** Paul Scherrer Institute, 5232 Villigen PSI, Switzerland, E-mail: stephan.heinitz@psi.ch
Emilio A. Maugeri, Dorothea Schumann, Rugard Dressler and Niko Kivel: Paul Scherrer Institute, 5232 Villigen PSI, Switzerland
Carlos Guerrero: Universidad de Sevilla, Av. Reina Mercedes, 41012 Sevilla, Spain
Ullrich Köster: Institut Laue-Langevin, 71 Av. de Martyrs, 38042 Grenoble, France
Moshe Tessler and Michael Paul: The Hebrew University of Jerusalem, 91904 Jerusalem, Israel
Shlomi Halfon: Soreq Nuclear Research Center, 81800 Yavne, Israel

Both prepared targets were measured at the n_TOF CERN facility in 2014 and 2015 and reliable cross section data were obtained for both isotopes for the first time. Additionally, a measurement of the corresponding Maxwellian average cross section was performed with the same targets at the LiLiT Soreq Applied Research Accelerator Facility (SARAF), Israel, in 2016 [11].

Cross section measurements demand high chemical and radioisotopic purity of the investigated isotope, since any interfering contaminant might deteriorate the quality of measured data. In order to obtain the desired radioisotope ${}^{A}_{Z}N$ in non-carrier-added form, neutron capture of a precursor seed ${}^{A-1}_{Z-1}N$ towards ${}^{A}_{Z-1}N$ with subsequent β^--decay is required. The material under irradiation needs a high enrichment grade and should be low in contamination for high production yields avoiding undesired side-products. Such a production pathway ensures very high isotopic purity of the desired material. Thus, the isotopes of ^{147}Pm and ^{171}Tm are most conveniently produced by neutron irradiation of ^{146}Nd and ^{170}Er in a high flux reactor, in analogy to the s-process depicted in Figure 1. After decay of ${}^{A}_{Z-1}N$, the irradiation results in a mixture of the isotopes ${}^{A-1}_{Z-1}N$, ${}^{A}_{Z}N$ and ${}^{A}_{Z+1}N$, and a sophisticated chemical separation of the final product from macroscopic amounts of the irradiated material is mandatory.

In order to fulfil this task, several approaches have been reported in literature. The separation of lanthanides was achieved by fractional crystallization [12], liquid–liquid extraction [13] and ion chromatography. The latter relies frequently on the use of standard cation exchange resins with organic acids as complexing agents. This method is most commonly used to achieve a sophisticated separation of neighboring lanthanides and actinides [9, 14–18]. Another approach is the use of the lanthanide specific exchange resin from TRISKEM, France, where a stepwise elution of the lanthanides is performed with mineral acids such as HNO_3. We have chosen a two-step chromatographic separation scheme involving a strong cationic exchange resin AMINEX (Bio-Rad, USA) followed by the lanthanide specific LN resin. The use of the former for the first separation has the following advantages:

- this high capacity cation exchanger allows the separation from large amounts of feed material up to 100 mg
- the separation performance of the AMINEX resin is substantially superior to similar cation exchange resins (e. g. Dowex AG 50 × 8) [19] using 2-hydroxy-isobuturic acid (α-HIBA) as complexing agent [20]
- the separation allows to elute the microscopic amounts of the product prior to the macroscopic amount of the educt, which significantly reduces contamination issues due to tailing effects [21]

The advantage to use the LN resin in the second separation step is three-fold:

- the complexing agent α-HIBA may easily be stripped off from this column
- the resin is commonly used for the separation of lanthanides for small amounts of material, thus even further increasing the separation efficiency from neighboring lanthanides
- the elution profile is inverse to that of the AMINEX resin. This circumstance allows separating contaminants still present in the product after the first separation

Especially the last named point represents a crucial advantage for performing a two-step separation scheme involving the AMINEX and the LN resin. Elements that have higher affinity towards the mobile phase and thus elute before the desired lanthanide, might be prone to tailing effects (e. g. Sc^{3+}, Ti^{4+}, Fe^{3+}, Zr^{4+}, Nb^{5+} Hf^{4+}) hence contaminating the later eluted product [22]. These elements have

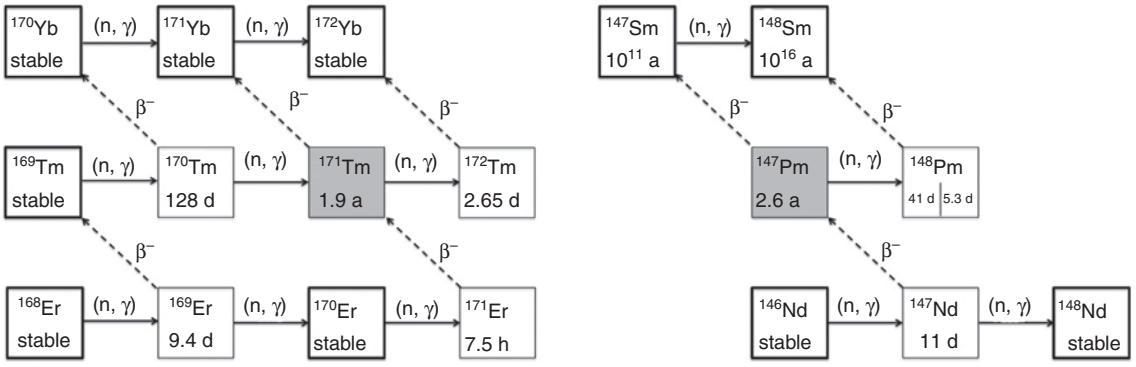

Figure 1: Production and destruction pathways during the stellar s-process for nuclides with mass number A = 171 and A = 147.

either higher ionic charge or smaller atomic radius than the lanthanides, thus forming stronger complexes with α-HIBA [23]. This property, on the contrary, delays their elution on the LN resin compared to lanthanides due to stronger affinity towards the stationary phase [24]. In analogy, elements with smaller ionic charge or larger ionic radius than the lanthanides (e. g. alkali and alkaline earth metals, transition metals) tend to be retained on the cation exchange resin. It has been shown that the elution of Mn^{2+}, Co^{2+} and Ni^{2+} from the resin with α-HIBA might coincide with the desired lanthanide element [25]. Nevertheless, these elements have low affinity towards the LN resin. Thus, even if there is a contamination by a certain unwanted stable or radioactive element after the first separation, a second separation involving an inverse elution sequence assures a clean product.

2 Experimental

2.1 Isotope production

The isotopes ^{171}Tm and ^{147}Pm were produced by thermal neutron irradiation at the high flux reactor of Institut Laue-Langevin (ILL), Grenoble, France. $^{170}Er_2O_3$ enriched to 98.1 % and $^{146}Nd_2O_3$ enriched to 98.8 % were purchased from Eurisotop, France. The isotopic composition and impurity content as stated by the supplier are given in Table 1.

One pellet of $^{170}Er_2O_3$ weighing 238.2 mg and two of $^{146}Nd_2O_3$ weighing in total 98.2 mg were produced using a hydraulic press, Portman Instruments, Switzerland. Each pellet was then encapsulated in air into a high purity quartz ampoule provided by WISAG AG, Switzerland, which was sealed by a flame torch. These ampoules were then irradiated at ILL for a period of 53.75 days with an average neutron flux of 8×10^{14} n cm^{-2} s^{-1}. An analytic calculation using published cross sections was performed to estimate the nuclide inventory. After a cooling period of approximately 1.5 years, the samples were shipped to PSI where they underwent chemical processing.

Table 1: Isotopic composition of Er and Nd as provided by the supplier.

Isotope[a]	Rel. abundance (%)	Isotope[b]	Rel. abundance (%)
^{162}Er	0.01	^{142}Nd	0.18
^{164}Er	0.03	^{143}Nd	0.14
^{166}Er	0.54	^{144}Nd	0.32
^{167}Er	0.38	^{145}Nd	0.24
^{168}Er	0.94	^{146}Nd	98.80
^{170}Er	98.10	^{148}Nd	0.24
		^{150}Nd	0.08

Impurities as stated by the supplier, ppm:

[a]Tm – 400, Gd – 400, Ca – 250, Ce – 160, Dy – 100, Yb – 90, Sm – 40.

[b]Pb – 46, Cu – 4, Er – 2, Gd – 2, La, Lu < 10.

2.2 Measurement techniques

2.2.1 ICP-MS

The determination of the isotopic composition as well as the concentration of ^{171}Tm and ^{147}Pm in the respective sample was performed by inductively coupled plasma – mass spectrometry (ICP-MS). Two sector-field-based mass spectrometers (Neptune and Element 2, Thermo Fisher Scientific, Bremen, Germany) were used. Both systems were operated in low-resolution mode and wet plasma conditions. All measurement solutions were prepared from high purity nitric acid and water in polymer vessels. After the determination of the isotopic composition, the concentration of the ^{171}Tm sample was determined by the isotope dilution method while the concentration of ^{147}Pm was quantified by standard addition. Standard solutions bearing 10 mg/L of Tm, Yb and Sm (ESI, Omaha, NE, USA) were used. Each of the prepared measurement solutions was measured four times.

In this work, the uncertainties are stated as combined standard uncertainties with a coverage factor of k = 1 and are estimated according to the "guide to the expression of uncertainty in measurement" (GUM).

2.2.2 γ-Ray spectrometry

γ-Ray spectrometric measurements at PSI were performed using a calibrated HPGe detector from Canberra GmbH, Germany. The Genie2000 software, Canberra, was used to evaluate the recorded spectra. Each sample was measured for at least 10 min to provide a statistical uncertainty below 1 % for the peak area of interest.

The final targets of ^{171}Tm and ^{147}Pm were measured at SARAF, Israel, at a distance of 777 cm and 50 cm, respectively, with a coaxial HPGe ORTEC GMX25-83 detector having 25 % relative efficiency and a 0.5 mm thin Be-window suitable for low energy γ-ray spectrometry. All targets and sources were enclosed in Al containers as used for experiments at LiLiT with an Al thickness of 1 mm facing the target. An efficiency calibration of the HPGe detector was made at relevant energies using the following set of

nuclides – ^{22}Na, ^{57}Co, ^{60}Co, ^{88}Y, ^{133}Ba, ^{137}Cs, ^{152}Eu, ^{155}Eu and ^{241}Am. The detector efficiency was determined to be constant in the energy range between 40 keV and 140 keV.

For the determination of the total activity of ^{171}Tm, the 66.73 keV γ-line with 0.143 % emission probability ([26], no uncertainty stated) was used. The detector was calibrated against a ^{241}Am source (408 kBq ± 1.7 % on the 01.06.1976, by The Radiochemical Centre, Amersham, UK) at 100 cm and 137 cm positioned in an Al container identical to that of ^{171}Tm. A correction for the scaling of efficiency with distance was applied and checked by the ^{241}Am measurements at both distances. In addition, a correction for the attenuation in Al and in air was made for ^{171}Tm and ^{241}Am counting.

For ^{147}Pm, the 121.22 keV line having an emission probability of 2.85×10^{-5} with 3.9 % uncertainty [27] was analysed with the same detector additionally placing 2 cm of Pb between source and detector [11]. The detector shielded in this kind was calibrated using a ^{57}Co source (378.1 kBq ± 1 % on the 01.11.2011, by Eckert&Ziegler, USA) at the same distance as the ^{147}Pm target. Owing to almost equal γ-ray energies and same distances in Al, Pb and in air, no correction was needed for the ^{57}Co calibration.

2.2.3 Liquid scintillation counting

A Tri-Carb CA2110 scintillation counter, Packard, USA, was used for liquid scintillation counting measurements. Aliquots of the ^{171}Tm sample were mixed with 10 mL of Aqua-Safe 500 Plus, provided by Zinsser Analytics, Germany, and measured for 60 min with automatic background subtraction.

Cherenkov measurements were performed with the same counter by mixing aliquots of the Tm solution with 10 mL of H_2O. Deionized water with a resistivity >18 MΩ cm was provided by an in-house deionized water purification system using Barnstead E-pure Ultrapure Water Purification Systems, Thermo Fisher Scientific, USA. For the determination of the ^{170}Tm Cherenkov counting efficiency, 0.1 mg of ^{169}Tm was irradiated at the PSI neutron activation facility to produce approx. 250 kBq ^{170}Tm. The irradiated material was dissolved in 0.5 mL of 0.01 M HNO_3 and Cherenkov and LSC solutions containing 10, 40 and 100 µL of the ^{170}Tm solution were prepared by mixing with 10 mL H_2O and 10 mL Aquasafe 500 Plus, respectively. The absence of interfering radioactive impurities was checked using γ-ray spectrometry. A re-measurement of all solutions was performed after 167 days to ensure the stability of the solutions and consistency of the detection efficiency.

2.3 Isotope separation

To avoid any health hazards by radioactivity due to dust formation, the ampules were crushed in a sealed polyethylene tube by a mechanical squeezer operated in a hotcell. The tube was then introduced into a dissolution apparatus, where 5 mL of hot 7 M HNO_3, Sigma Aldrich, Switzerland, from a heated 10 mL V-vial was pumped into the tube. A graphical representation of the experimental apparatus is given in Figure 2. Afterwards the solution was pumped back into the V-vial, whereas a micro-pore filter within the tube assured that no glass residue is transferred with the solution. The back-and-forth pumping operations were repeated at least 15 times until a complete dissolution of the pellets was visually confirmed. The glass residues were then washed three times with 1 mL of H_2O.

The acidic solution containing the dissolved lanthanides was then evaporated to near-dryness by blowing nitrogen over the heated solution overnight. After addition of 5 mL H_2O the solution was pumped from the V-vial into a 50 mL Pyrex glass flask with subsequent washing of the V-vial, the glass residues and the tubes with another 45 mL of H_2O. The pH of the combined solution, approx. 50 mL in volume, was adjusted to pH = 4 with diluted ammonia.

In order to qualitatively observe and quantify the elution of the lanthanides, γ-ray spectrometry as described in Section 2.2 was applied. In order to monitor the elution of these elements during separation, γ-active tracers were produced at PSI by neutron activation. Before every separation of Tm from Er, 1.0 mg of inactive $^{170}Er(NO_3)_3$ had been irradiated with 10^{13} n cm^{-2} s^{-1} for 3600 s to produce ^{171}Er, which was immediately dissolved in 1 mL H_2O and transferred into the stock solution. For the separation of ^{147}Pm, 2.5 mg of inactive $^{146}Nd_2O_3$ was placed in a quartz ampoule, sealed with a flame-torch and irradiated for 5 days with 4×10^{13} n cm^{-2} s^{-1} to produce ^{147}Nd two months prior to use. After irradiation, the Nd oxide was dissolved in 4 M HNO_3, the solution evaporated, the residue re-dissolved in 2 mL of H_2O and added to the Nd stock solution.

The separation of lanthanides was performed on a strong cation exchange resin Aminex HPX87H, 9 µm particle size, 1.77 Meq H^+/g, provided by Bio-Rad Laboratories, USA. The resin was transferred into a glass column with dimensions of 1 cm diameter and 25 cm length. Prior to any separation, the resin was thoroughly washed with 4 M TRACEPUR HNO_3 provided by Sigma Aldrich, Switzerland, and then transformed into the NH_4^+ form using 1 M NH_4NO_3 until a near neutral pH of the effluent was reached. The initial solutions of ^{171}Tm and ^{147}Pm were pumped via a peristaltic pump ISM834C provided by Ismatec, Switzerland, onto the

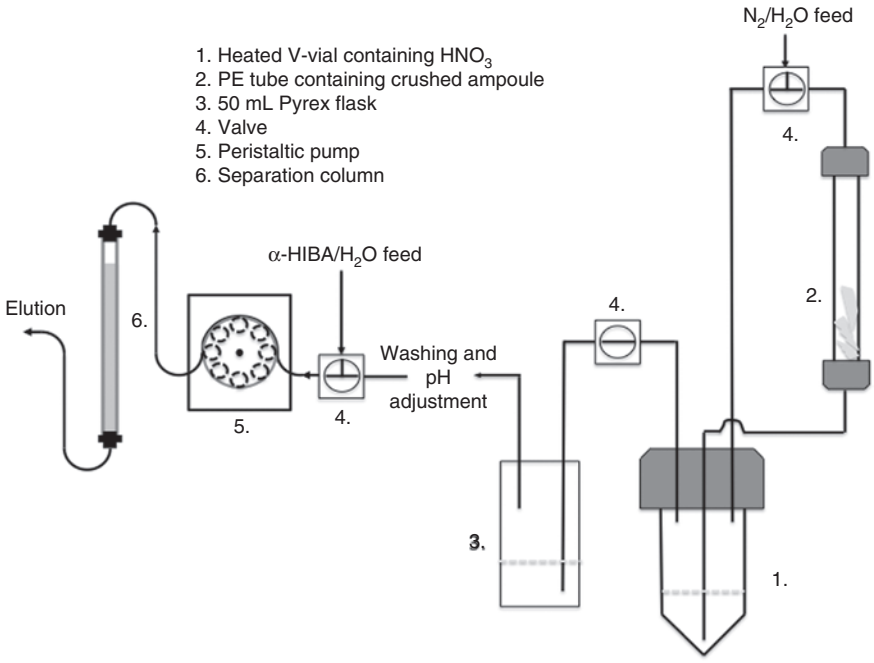

Figure 2: Experimental scheme for dissolution and separation of irradiated Er and Nd samples.

column to achieve a loading of approx. 50 mg of either Er or Nd. The column was then washed with 20 mL of H_2O.

The elution of the lanthanides was performed at room temperature using increasing concentrations of α-HIBA. Solutions ranging from 0.05 M up to 1 M α-HIBA at pH = 4.40 were prepared by dissolving the corresponding mass of the organic acid provided by Fluka, Switzerland, in 1 L of deionized H_2O. The pH was adjusted with ammonia solution using a S20 SevenEasy™ pH-meter, Mettler-Toledo, Switzerland. For the elution of Tm the α-HIBA concentration was 0.075 M, while for the elution of Pm the concentration was 0.25 M. The flow rate was adjusted to 0.5 mL/min and fractions containing 10 mL of solution were collected in 20 mL PE-vials and immediately measured via γ-ray spectrometry. The activity in the effluent passing through a thin tube connected to the bottom of the column was continuously monitored with an end-window GM counter. In order to subsequently elute all radioisotopes present on the column, a steady increase in α-HIBA concentration to 1 M was maintained until there was no detectable activity staying on the column. After each separation, the column was washed with 4 M HNO_3 and 1 M NH_4NO_3 to be prepared for the next separation. In total, five subsequent separations were performed for ^{171}Tm, while ^{147}Pm was separated in two runs.

All fractions containing radiochemically pure ^{171}Tm or ^{147}Pm were combined and the solutions acidified with ¼ the volume of 1 M HNO_3. The solutions were then loaded on a 20 cm long, 1 cm dia. column filled with LN resin, 100 µm–200 µm particle size, provided by Triskem International, France. During loading of the column, no breakthrough of the radioisotope was observed. After washing with 100 mL of 0.1 M HNO_3, the elution of ^{171}Tm was performed with 3 M HNO_3, TRACEPUR grade, Sigma-Aldrich, Switzerland. For the elution of ^{147}Pm, 0.25 M HNO_3 of the same HNO_3 grade was used.

After merging the eluted fractions, an aliquot of 450 µL weighing 451 mg was taken from 20.038 g of the ^{171}Tm solution to be measured by ICP-MS. The aliquot was then diluted 1:100 using distilled water and used for measurements involving γ-ray spectrometry, liquid scintillation counting and ICP-MS. Similarly, a 50 µL aliquot weighing 49.1 mg was taken from 22.1837 g of the ^{147}Pm solution and was measured by ICP-MS.

In addition, samples of the eluted fractions of radiochemically pure Yb/Sm and Er/Nd were collected for the determination of their isotopic composition via ICP-MS.

2.4 Target preparation

The method of choice for the preparation of radioactive targets for n_TOF CERN was molecular plating. Target preparation was identical for ^{171}Tm and ^{147}Pm. The purified radioisotope solutions were evaporated in a thoroughly cleaned quartz beaker under a nitrogen stream.

The evaporated residue containing the radioactive isotope was re-dissolved in 100 µL of 0.01 M HNO_3 and 2 mL of 2-propanol, provided by Sigma-Aldrich, Switzerland, was added. Half of this solution was then transferred into the molecular plating cell and further 9 mL of 2-propanol were added. The deposition cell consisted of a Pt wire anode inserted in a 50 mL machined polyvinylidene fluoride (PVDF) vessel with a Cu cathode at its bottom. The molecular plating was performed for 1 h applying a voltage of 350 V at currents ranging from 10 mA to 30 mA. Two 5 µm thick Al foils obtained from Robert Victor Neher AG, Switzerland, with a diameter of 27 mm were used as deposition substrate. After deposition, the solution from the deposition cell was transferred into the initial evaporation vial to be mixed with the second half of the material. The first foil with the deposit was removed from the deposition cell, dried and a second deposition was done with the rest of the material as described above. After drying, both foils were prepared for the final target assembly.

Two 6 µm Mylar® polyester film foils provided by DuPont Teijin Films, UK, were glued on two glass-fiber reinforced plastic rings (d_{out} = 60 mm, d_{in} = 50 mm) representing the target frame. The Al foils containing the radioisotope were centrally positioned on one such frame face-to-face with the active deposit pointing inwards. The second frame was then placed above the stack and both Mylar® foils were glued circularly to each other by pressing them together with a Cu ring, 40 mm in diameter, heated to 120 °C. As such, the sandwich-like structure represented a closed source containing the radioisotope suitable for n_TOF experiments. All operations were performed in a sealed, inflatable AtmosBag provided by Sigma Aldrich, Switzerland, to avoid any contamination issues. The dose rate at 10 cm distance was 1.5 mSv/h for the ^{171}Tm target and 20 µSv/h for the ^{147}Pm target.

In order to assess the deposition efficiency, the remaining solution containing non-deposited ^{171}Tm and ^{147}Pm in 2-propanol was evaporated to dryness and 10 mL of 0.01 M HNO_3 was added. An aliquot was taken from each solution for the determination of the deposition efficiency using γ-ray spectrometry, liquid scintillation and ICP-MS.

3 Results

3.1 Separation performance

Measurements via γ-ray spectrometry of the initial solutions revealed the presence of the following radioisotopes in the sample of ^{170}Er: ^{46}Sc, ^{60}Co, ^{65}Zn, ^{114m}In, ^{145}Sm, ^{154}Eu, ^{153}Gd, ^{160}Tb, ^{166m}Ho, $^{170/171}$Tm, ^{192}Ir. The sample of ^{146}Nd contained ^{46}Sc, ^{60}Co, ^{65}Zn, ^{110m}Ag, ^{139}Ce, ^{147}Pm, ^{145}Sm, $^{154/155}$Eu, ^{160}Tb and $^{170/171}$Tm. The elution profile for one of the five subsequent separations of ^{171}Tm from Er is given in Figure 3. Evidently, substantial amounts of other radiotracers were present in the irradiated sample and could successfully be separated by ion chromatography. Each separation run

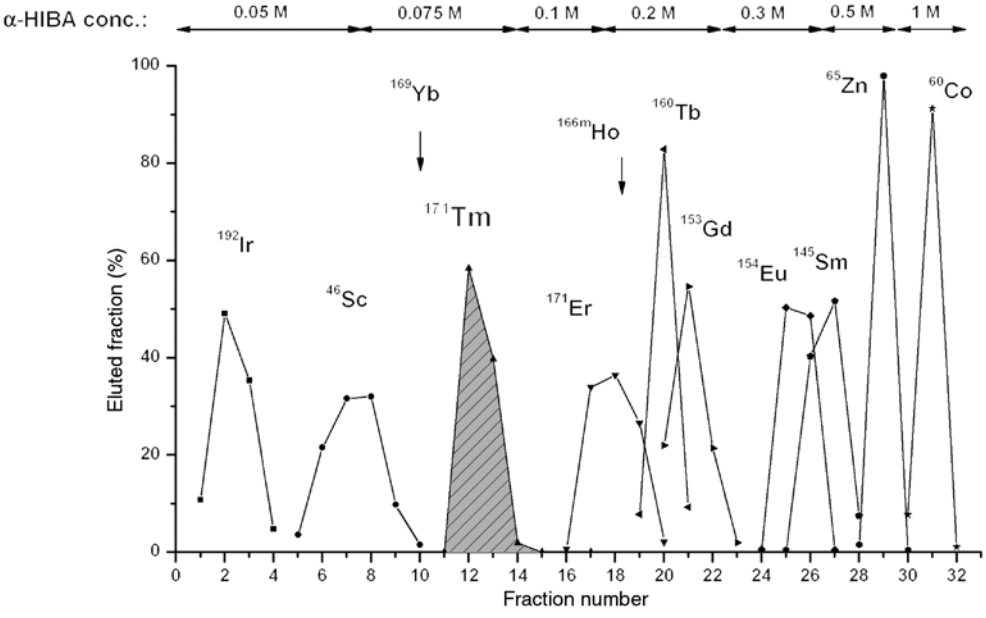

Figure 3: Separation profile of ^{171}Tm on the Aminex HPX87H cation resin. The gradual elution of different radioisotopes with increasing α-HIBA concentration is shown.

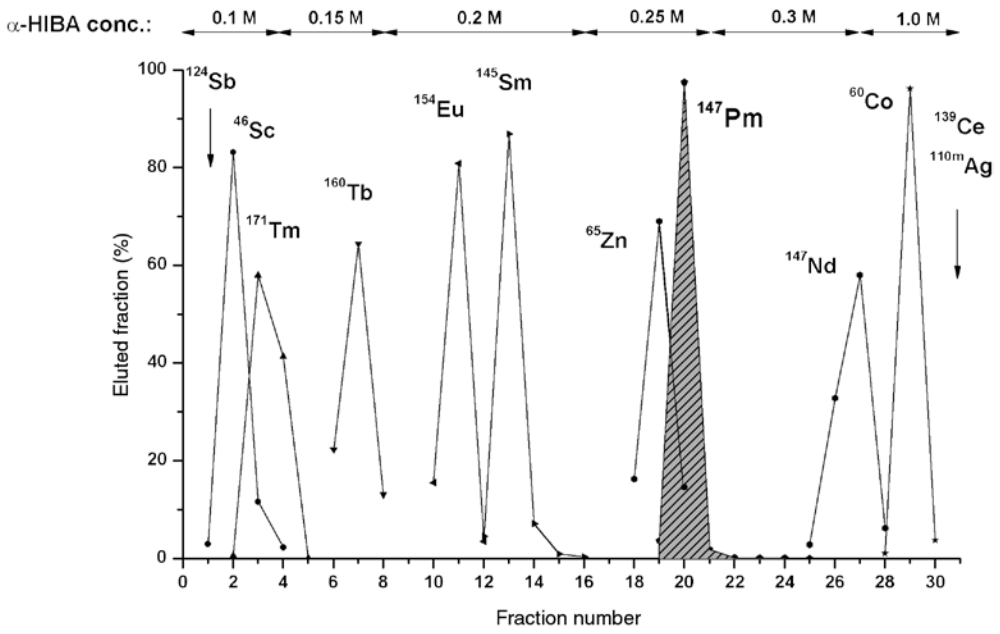

Figure 4: Separation profile of ^{147}Pm on the Aminex HPX87H cation resin. The gradual elution of different radioisotopes with increasing α-HIBA concentration is shown.

gave a very similar elution profile, hence no degradation of the column performance was observed. The separation profile for ^{147}Pm is given in Figure 4. It is noteworthy that the elution of ^{65}Zn coincided with the one for ^{147}Pm. The second separation involving the LN resin allowed separating the unwanted activity of ^{65}Zn, which was eluted using 0.01 M HNO_3 without any breakthrough of ^{147}Pm before its elution with 0.25 HNO_3. ^{171}Tm was eluted with 3 M HNO_3 and small amounts of ^{46}Sc remained on the column.

The characterization of the isotopic composition of the Tm sample after separation as well as the corresponding Yb and Er fraction is given in Table 2. As can be seen, the major signal contributions in the final Tm sample stem from mass 169, 170 and 171; signals at other masses were close to the detection limit of the spectrometer. Because isobaric interferences are not distinguishable by ICP-MS, a careful assignment of the measured signals has to be undertaken.

Table 2: Isotopic composition of the final Tm product and the eluted element fractions of Yb and Er measured by ICP-MS.

Mass (m/q)	Rel. isotopic abundance in fraction (%)		
	Tm	Yb	Er
168	1×10^{-3}	<	1.41
169	2.03	<	<
170	0.06	1.73	98.02
171	97.91	90.70	<
172	<	2.70	<
173	8×10^{-4}	4.67	<

Values denoted by "<" were below the detection limit of the spectrometer.

Since no ^{169}Yb could be detected by γ-ray spectrometry in the final product, the contribution at mass 169 is only attributed to stable ^{169}Tm. The signal contributions to mass 168 and 173 may not originate from the respective Tm isotopes, since neither ^{168}Tm nor ^{173}Tm could be detected by γ-ray spectrometry. Thus, these signals are attributed to the stable contaminants ^{168}Er and ^{173}Yb, respectively. According to the measured isotopic composition of Yb and Er in the final Tm product given in Table 2, the relative contribution of these two contaminants to the Tm signal at masses 170 and 171 was calculated. While ^{171}Yb contributes to 0.016 % of signals at mass 171, the signal at mass 170 originates from three different isobars: the impurities of ^{170}Yb and ^{170}Er as well as the radioactive isotope ^{170}Tm. Based on data from Cherenkov counting and ICP-MS, the contribution of the last named Tm isotope to mass 170 is approx. 85 %, while the rest is mainly attributed to ^{170}Er, resulting in a maximum content of Yb of 170 ppm and of Er of 70 ppm in the final ^{171}Tm product. The higher abundance of ^{173}Yb compared to ^{172}Yb is noteworthy, giving some argument to suggest a high burn-up rate in the A = 172 mass region.

Table 3 denotes the relative isotopic abundances measured in the collected fractions of Pm, Sm and Nd. The data given for the final Pm sample indicates a product

Table 3: Isotopic composition of the final Pm product and the eluted element fractions of Sm and Nd; measured by ICP-MS.

Mass (m/q)	Rel. isotopic abundance in fraction (%)		
	Pm	Sm	Nd
145	<	0.01	0.21
146	0.10	0.31	98.74
147	99.45	60.96	<
148	7.1×10^{-3}	13.78	0.32
149	<	1.57	<
150	6.1×10^{-3}	16.87	0.10

of high isotopic purity. Minor contaminations are observable at masses 146, 148 and 150. The signal at mass 146 is attributed solely to a ^{146}Nd impurity, since only roughly 100 Bq of ^{146}Pm could be detected by γ-ray spectrometry in the final product. Signal contributions at mass 148 and 150 are attributed to the corresponding Sm isotopes. According to numbers given in Table 3, the total Nd and Sm content in the final ^{147}Pm product was derived to be 1050 and 440 ppm, respectively.

3.2 Deposition performance

The final deposition efficiency for the ^{171}Tm target was determined to be 93.6 ± 0.4 %, which represents the mean value of four independent measurements of aliquots taken before and after molecular plating with ICP-MS, γ-ray spectrometry, LSC and Cherenkov counting. The total amount of Tm isotopes produced by irradiation was in excellent agreement with activation estimations done with thermal neutron capture cross sections reported in literature.

The deposition efficiency for the ^{147}Pm target was determined to be 50.2 ± 2.4 % according to γ-ray spectrometry, that is significantly lower than was achieved for molecular plating of ^{171}Tm. The reason for such a behaviour is hard to assess, since no test depositions could be performed for Pm as was the case for Tm, due to the lack of a stable Pm isotope. Presumably, the much lower quantity of Pm was more sensitive to relevant plating parameters, e. g. the applied voltage or deposition current.

The final evaluation of the total amount of ^{147}Pm produced during irradiation revealed that only 60 % of the material was obtained compared to the calculated prediction. A possible reason for this discrepancy is the higher burnup of produced ^{147}Nd during irradiation compared to theory. The activation estimate was performed with a ^{147}Nd(n, γ)^{148}Nd cross section of 49 b, while a recent evaluation indicates that this value is a factor of five higher [28].

3.3 Target characterization

The total amount of Tm and Pm deposited on each pair of Al backings is summarized in Tables 4 and 5. Due to possible material loss during target assembly, the total amount of ^{147}Pm and ^{171}Tm was determined based on the γ-ray spectrometric analysis of both final targets performed at SARAF on the 24.11.2016. All data refer back to the date of the final separation on the LN resin, which was 01.11.2014 in case of ^{171}Tm and 07.05.2015 in case of ^{147}Pm, using their reported half-lives of 1.92(1) a [26] and 2.6234(4) a [27], respectively. Additionally taking into account data given in Tables 2 and 3, the decontamination factor for Tm from Er is calculated to be at least 7×10^5, while it is 5×10^5 for the Nd/Pm pair.

Due to the ^{168}Er(n, γ) reaction occurring during irradiation, there is always stable ^{169}Tm present, which by subsequent neutron capture also yields ^{170}Tm. The Cherenkov counting technique was able to determine the content of ^{170}Tm despite the much higher activity of ^{171}Tm present, since the latter isotope is not detectable by this technique. The measurement yielded a total activity of 400 MBq of ^{170}Tm in the target, which is in good agreement to data given in Table 4. The uncertainty estimation stems from tension between Cherenkov data and the upper limit

Table 4: Main isotope content of the ^{171}Tm target on the reference date 01.11.2014.

Isotope	^{171}Tm	^{170}Tm	^{169}Tm
Atoms	*1.23×10^{19}*	*7.4×10^{15}*[b]	*2.59×10^{17}*[b]
Activity (Bq)	1.40×10^{11}[a]	*4.6×10^{8}*	–
Mass (µg)	*3480*	*1.9*	*72.7*
Uncertainty (%)	2.4	20	3

Numbers given in italic are calculated according to the activity measurement of ^{171}Tm.
[a]Determined by γ-ray spectrometry at SARAF. [b]Calculated according to ICP-MS atomic ratios.

Table 5: Main isotope content of the ^{147}Pm target on the reference date 07.05.2015.

Isotope	^{147}Pm	^{146}Nd	^{147}Sm
Atoms	*2.96×10^{17}*	*3.1×10^{14}*[b]	*1.3×10^{14}*[b]
Activity (Bq)	2.48×10^{9}[a]	–	–
Mass (µg)	*72.2*	*0.08*	*0.03*
Uncertainty (%)	4.3	12	35

Numbers given in italic are calculated according to the activity measurement of ^{147}Pm.
[a]Determined by γ-ray spectrometry at SARAF. [b]Calculated according to ICP-MS atomic ratios.

determined by γ-ray spectrometry. The Cherenkov detection efficiency for the ^{170}Tm isotope was determined using scintillation counting to be 14.95 ± 0.15 %, in agreement with theoretical data [29].

The corresponding spectrum of the ^{171}Tm target is shown in Figure 5 together with the ^{241}Am calibration.

The characterization of the ^{147}Pm target is given in Table 5. On the reference date 07.05.2015, the target had a ^{147}Pm activity of 2.48 GBq. It also contains the isotopes of $^{143, 144, 146, 148, 148m}$Pm, with ^{148m}Pm having the highest activity of roughly 3 kBq on the separation date – which corresponds, by atom number, to well below 10^{11} atoms or <1 ppm for each of the listed Pm isotopes. The only major contaminant is ^{145}Pm, originating from decay of its mother ^{145}Sm that is produced during irradiation of Sm impurities, namely the ^{144}Sm isotope. The assessment of the total activity of ^{145}Sm after chemical purification revealed that approx. 80 kBq of ^{145}Pm should have been formed by ^{145}Sm decay during the cooling period of the irradiated sample. This corresponds to roughly 100 ppm of ^{145}Pm in the final ^{147}Pm target. The corresponding γ-ray spectrum of the ^{147}Pm target together with the used ^{57}Co calibration source is given in Figure 6.

The final assembly for the ^{171}Tm target delivered to n_TOF CERN is given in Figure 7. A similar target was prepared in the case of ^{147}Pm. Both targets were measured in 2014 and 2015 immediately on arrival in order to minimize the contribution of the ingrowing daughter nuclides of ^{171}Yb and ^{147}Sm, respectively. The data of these measurements are currently being analysed and first results are published in [30].

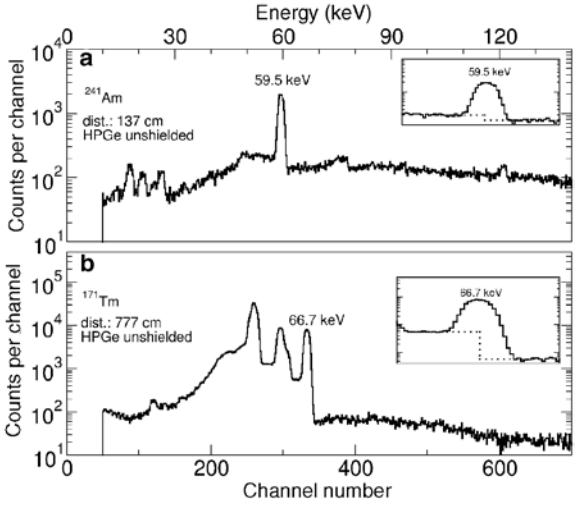

Figure 5: Recorded γ-ray spectra for (a) the ^{241}Am calibration source and (b) the ^{171}Tm target showing their respective γ-ray emission peaks at 59.5 and 66.7 keV measured at SARAF on 24.11.2016.

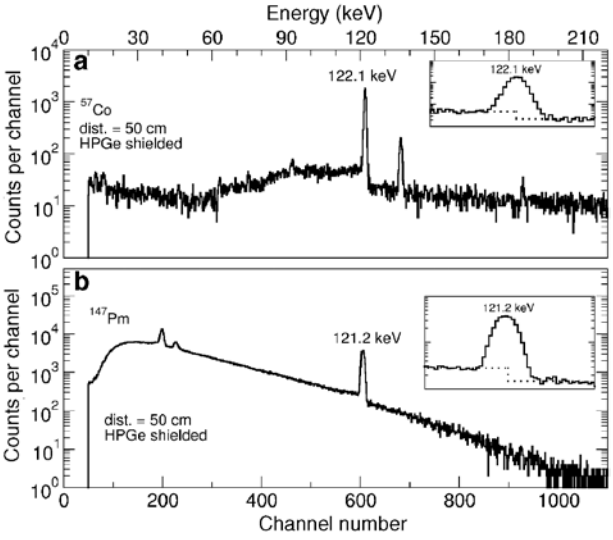

Figure 6: Recorded γ-ray spectra for (a) the ^{57}Co calibration source and (b) the ^{147}Pm target with their respective emission lines of 122.1 and 121.2 keV, respectively; measured at SARAF on 24.11.2016.

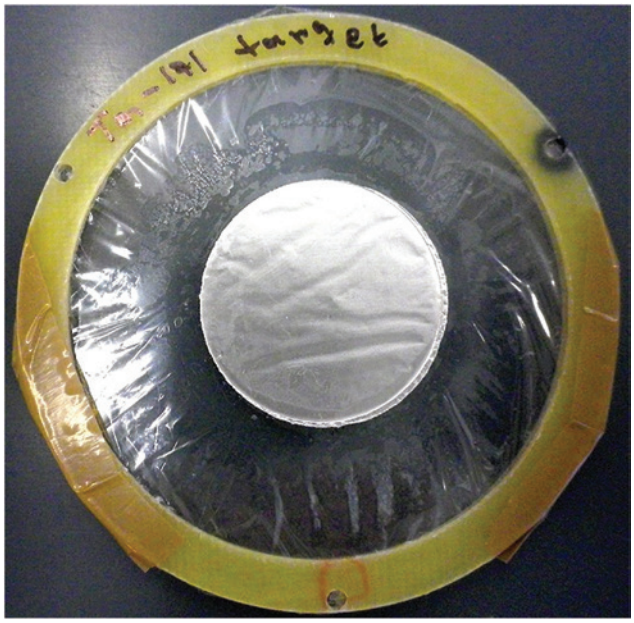

Figure 7: The final arrangement of the ^{171}Tm target provided to n_TOF CERN.

4 Summary

We have successfully separated 140 GBq ^{171}Tm and 2.5 GBq ^{147}Pm from hundreds of milligrams of irradiated, enriched lanthanide seed materials. Two suitable targets containing the separated radioisotopes were successfully prepared by molecular plating and provided to n_TOF CERN

and to the SARAF-LiLiT facility for neutron cross-section measurements.

The combination of two different consecutive separation columns has proven to be a very powerful technique to achieve high decontamination factors from neighboring lanthanides. For the Tm/Er pair we achieved a decontamination factor of 7×10^5 while for the Pm/Nd pair it was 5×10^5. The final products had a high isotopic and chemical purity.

This separation procedure might be adopted for further lanthanide separations required for radioactive targets of high purity involving, for example ^{163}Ho and ^{155}Eu. These separations are a prerequisite for the feasibility of future neutron TOF measurements on unstable branching point isotopes for astrophysical research.

Acknowledgments: The authors are grateful to A. Vögele in performing neutron activation of various lanthanide samples during this work. Advices and help of E. Schaub and H. Dorrer during planning and construction of the separation setup are highly appreciated. This measurement has received funding from the EC FP7 Program under the projects NEUTANDALUS (Grant No. 334315) and CHANDA (Grant No. 605203).

References

1. Burbidge, E. M., Burbidge, G. R., Fowler, W. A., Hoyle, F.: Synthesis of the elements in stars. Rev. Mod. Phys. **29**(4), 547 (1957).
2. Kaeppeler, F., Gallino, R., Bisterzo, S., Aoki, W.: The s process: nuclear physics, stellar models, and observations. Rev. Mod. Phys. **83**(1), 157 (2011).
3. Abbondanno, U., Aerts, G., Álvarez-Velarde, F., Alvarez-Pol, H., Andriamonje, S., Andrzejewski, J., Badurek, G., Baumann, P., Bečvář, F., Benlliure, J., Berthoumieux, E., Calvino, F., Cano-Ott, D., Capote, R., Cennini, P., Chepel, V., Chiaveri, E., Colonna, N., Cortes, G., Cortina, D., Couture, A., Cox, J., Dababneh, S., Dahlfors, M., David, S., Dolfini, R., Domingo-Pardo, C., Duran, I., Embid-Segura, M., Ferrant, L., Ferrari, A., Ferreira-Marques, R., Frais-Koelbl, H., Furman, W., Goncalves, I., Gallino, R., Gonzalez-Romero, E., Goverdovski, A., Gramegna, F., Griesmayer, E., Gunsing, F., Haas, B., Haight, R., Heil, M., Herrera-Martinez, A., Isaev, S., Jericha, E., Kappeler, F., Kadi, Y., Karadimos, D., Kerveno, M., Ketlerov, V., Koehler, P., Konovalov, V., Krticka, M., Lamboudis, C., Leeb, H., Lindote, A., Lopes, I., Lozano, M., Lukic, S., Marganiec, J., Marrone, S., Martinez-Val, J., Mastinu, P., Mengoni, A., Milazzo, P. M., Molina-Coballes, A., Moreau, C., Mosconi, M., Neves, F., Oberhummer, H., O'Brien, S., Pancin, J., Papaevangelou, T., Paradela, C., Pavlik, A., Pavlopoulos, P., Perlado, J. M., Perrot, L., Pignatari, M., Plag, R., Plompen, A., Plukis, A., Poch, A., Policarpo, A., Pretel, C., Quesada, J., Raman, S., Rapp, W., Rauscher, T., Reifarth, R., Rosetti, M., Rubbia, C., Rudolf, G., Rullhusen, P., Salgado, J., Soares, J. C., Stephan, C., Tagliente, G., Tain, J., Tassan-Got, L., Tavora, L., Terlizzi, R., Vannini, G., Vaz, P., Ventura, A., Villamarin, D., Vincente, M. C., Vlachoudis, V., Voss, F., Wendler, H., Wiescher, M., Wisshak K.: Neutron capture cross section measurement of Sm-151 at the CERN neutron time of flight facility (n_TOF). Phys. Rev. Lett. **93**(16), 5 (2004).
4. Lederer, C., Massimi, C., Altstadt, S., Andrzejewski, J., Audouin, L., Barbagallo, M., Bécares, V., Bečvář, F., Belloni, F., Berthoumieux, E., Billowes, J., Boccone, V., Bosnar, D., Brugger, M., Calviani, M., Calviño, F., Cano-Ott, D., Carrapiço, C., Cerutti, F., Chiaveri, E., Chin, M., Colonna, N., Cortés, G., Cortés-Giraldo, M. A., Diakaki, M., Domingo-Pardo, C., Duran, I., Dressler, R., Dzysiuk, N., Eleftheriadis, C., Ferrari, A., Fraval, K., Ganesan, S., García, A. R., Giubrone, G., Gómez-Hornillos, M. B., Gonçalves, I. F., González-Romero, E., Griesmayer, E., Guerrero, C., Gunsing, F., Gurusamy, P., Jenkins, D. G., Jericha, E., Kadi, Y., Käppeler, F., Karadimos, D., Kivel, N., Koehler, P., Kokkoris, M., Korschinek, G., Krtika, M., Kroll, J., Langer, C., Leeb, H., Leong, L. S., Losito, R., Manousos, A., Marganiec, J., Martínez, T., Mastinu, P. F., Mastromarco, M., Meaze, M., Mendoza, E., Mengoni, A., Milazzo, P. M., Mingrone, F., Mirea, M., Mondelaers, W., Paradela, C., Pavlik, A., Perkowski, J., Pignatari, M., Plompen, A., Praena, J., Quesada, J. M., Rauscher, T., Reifarth, R., Riego, A., Roman, F., Rubbia, C., Sarmento, R., Schillebeeckx, P., Schmidt, S., Schumann, D., Tagliente, G., Tain, J. L., Tarrío, D., Tassan-Got, L., Tsinganis, A., Valenta, S., Vannini, G., Variale, V., Vaz, P., Ventura, A., Versaci, R., Vermeulen, M. J., Vlachoudis, V., Vlastou, R., Wallner, A., Ware, T., Weigand, M., Weiß, C., Wright, T. J., Zugec, P.: Neutron capture cross section of unstable Ni-63: implications for stellar nucleosynthesis. Phys. Rev. Lett. **110**(2), 022501 (2013).
5. Weigand, M., Bredeweg, T. A., Couture, A., Goebel, K., Heftrich, T., Jandel, M., Kaeppeler, F., Lederer, C., Kivel, N., Korschinek, G., Krticka, M., O'Donnell, J. M., Ostermöller, J., Plag, R., Reifarth, R., Schumann, D., Ullmann, J. L., Wallner, A.: Ni-63(n,gamma) cross sections measured with DANCE. Phys. Rev. C **92**(4), (2015).
6. Reifarth, R., Haight, R., Heil, M., Fowler, M. M., Käppeler, F., Miller, G. G., Rundberg, R. S., Ullmann, J. L., Wilhelmy, J. B.: Neutron capture measurements on Tm-171. Nucl. Phys. A **718**, 478 (2003).
7. Schwantes, J. M., Taylor, W. A., Rundberg, R. S., Vieira, D. J.: Preparation of a one-curie Tm-171 target for the detector for advanced neutron capture experiments (DANCE). J. Radioanal. Nucl. Chem. **276**(2), 533 (2008).
8. Gharibyan, N., Bene, B. J., Sudowe, R.: Chromatographic separation of thulium from erbium for neutron capture cross section measurements – part I: trace scale optimization of ion chromatography method with various complexing agents. J. Radioanal. Nucl. Chem. **311**(1), 179 (2016).
9. Bene, B. J., Taylor, W. A., Birnbaum, E. R., Sudowe, R.: Chromatographic separation of thulium from erbium for neutron capture cross section measurements – part II: preparative scale separation. J. Radioanal. Nucl. Chem. **311**(1), 155 (2016).
10. Reifarth, R., Arlandini, C., Heil, M., Käppeler, F., Sedyshev, P. V., Mengoni, A., Herman, M., Gallino, R., Travaglio, C.: Stellar neutron capture on promethium: implications for the s-process neutron density. Astrophys. J. **582**(2), 1251 (2003).
11. Tessler, M., Paul, M., Palchan, T., Halfon, S., Weissmann, L., Hazenshprung, N., Kreisel, A., Makmal, T., Shor, A., Silverman, I.: Nucleosynthesis reactions with the high-intensity SARAF-LiLiT neutron source. In: Proceedings of "The 26th International Nuclear Physics Conference", PoS (INPC2016) 139 (2017).

12. James, C.: Thulium I. J. Am. Chem. Soc. **33**, 1332 (1911).
13. Mokili, B., Poitrenaud, C.: Medium effect on the separation factor in liquid-liquid extraction. Application to the separation of trivalent lanthanide nitrates by tri-n-butylphosphate. Solv. Extr. Ion Exchange **15**(3), 455 (1997).
14. Nedjadi, Y., Bailat, C., Caffari, Y., Froidevaux, P., Wastiel, C., Kivel, N., Guenther-Leopold, I., Triscone, G., Jaquenod, F., Bochud, F.: A new measurement of the half-life of ^{166m}Ho. Appl. Rad. Isot. **70**(9), 1990 (2012).
15. Alexander, C. W., Halperin, J., Knauer, J. B., Walker, R. L.: The thermal-neutron capture cross-sections and resonance integrals of Sm-144 and Sm-145. Nucl. Sci. Eng. **95**(3), 194 (1987).
16. Gourgiotis, A., Isnard, H., Nonell, A., Aubert, M., Stadelmann, G., Dupont, E., AlMahamid, I., Tiang, G., Rao, L., Lukens, W., Cassettee, P., Panebiancob, S., Letourneaub, A., Chartierf, F.: Bk and Cf chromatographic separation and ^{249}Bk/^{248}Cm and ^{249}Cf/^{248}Cm elemental ratios determination by inductively coupled plasma quadrupole mass spectrometry. Talanta **106**, 39 (2013).
17. Qaim, S. M.: Measurement of (n,p) reaction cross-sections at 14.7 Mev using high-pressure liquid-chromatography in region of rare-earths. Radiochim. Radioanal. Let. **25**(5–6), 335 (1976).
18. Qaim, S. M., Ollig, H., Blessing, G.: Separation of lanthanides by preparative high-pressure liquid-chromatography. Radiochim. Acta **26**(1). 59 (1979).
19. Höhlein, G., Völler, H., Weinländer, W.: Verwendung von aminex* zur trennung von actiniden und lanthaniden. Radiochim. Acta **11**(3/4), 172 (1969).
20. Choppin, G. R., Silva, R. J.: Separation of the lanthanides by ion exchange with alpha-hydroxy isobutyric acid. J. Inorg. Nucl. Chem. **3**(2), 153 (1956).
21. Mocko, V., Taylor, W. A., Nortier, F. M., Engle, J. W., Barnhart, T. E., Nickles, R. J., Pollington, A. D., Kunde, G. J., Rabin, M. W., Birnbaum, E. R.: Isolation of ^{163}Ho from dysprosium target material by HPLC for neutrino mass measurements. Radiochim. Acta **103**(8), 577 (2015).
22. Perdue, H. D., Conover, A., Sawley, N., Anderson, R.: Chemical separations using alpha-hydroxyisobutyric acid solutions and both cation and anion exchange resin. Anal. Chem. **40**(12), 1773 (1968).
23. Martell, A. E.: Critical Stability Constants, Vol.3: Other Organic Ligands, Springer Science + Business Media, New York (1977).
24. Horwitz, E. P., Bloomquist, C.: Chemical separations for superheavy element searches in irradiated uranium targets. J. Inorg. Nucl. Chem. **37**(2), 425 (1975).
25. Borai, E., Ekhlom, P., Harjula, R.: Group separation of heavy metals followed by subsequent and individual separation of lanthanides by chelation chromatography. J. Liquid Chrom. Rel. Tech. **37**(11), 1614 (2014).
26. Baglin, C. M.: Nuclear data sheets for A = 171. Nucl. Data Sheets **96**(3), 399 (2002).
27. Nica, N.: Nuclear data sheets for A = 147. Nucl. Data Sheets **110**(4), 749 (2009).
28. Rochman, D., Leray, O., Perret, G., Vasiliev, A., Ferroukhi, H., Koning, A. J.: Re-evaluation of the thermal neutron capture cross section of ^{147}Nd. Annals Nucl. Energy **94**, 612 (2016).
29. Grau Carles, A., Grau Malonda, A.: CHEREN2, the Cherenkov counting efficiency by an anisotropy detection model. Comp. Phys. Comm. **174**(1), 30 (2006).
30. Guerrero, C., Domingo-Pardo, C., Lerendegui-Marco, J., Casanovas, A., Cortes-Giraldo, M. A., Dressler, R., Halfon, S., Heinitz, S., Kivel, N., Köster, U., Paul, M., Quesada-Molina, J. M., Schumann, D., Tarifeño-Saldivia, A., Tessler, M., Weissman, L. (The n_TOF and LiLiT Collaborations).: Neutron capture cross sections of the s-process branching points ^{147}Pm, ^{171}Tm, and ^{204}Tl. In: JPS Conf. Proc. 010903 (2017). https://doi.org/10.7566/JPSCP.14.010903.